LA-UR -91-1635

LA-UR--91-1635

DE91 013078

Los Alamos National Laboratory is operated by the University of California for the United States Department of Energy under contract W-7405-ENG-36

TITLE THE EXPERIMENTAL PROGRAM AT THE WNR NEUTRON SOURCE AT LAMPF

AUTHOR(S) P.W. Lisowski

SUBMITTED TO Proceedings for the "Specialists Meeting on Neutron Cross Section Standards for the Energy Range Above 20 MeV", Henri Conde, host, Uppsala, Sweden, 5/21-5/23/91

Los Alamos National Laboratory
Los Alamos, New Mexico 87545

MASTER

FORM NO 836 R4
ST NO 2629 5/81

THE EXPERIMENTAL PROGRAM AT THE WNR NEUTRON SOURCE AT LAMPF

P. W. Lisowski
Los Alamos National Laboratory
Los Alamos, NM, U.S.A.

There are two white neutron sources at Los Alamos National Laboratory which are used in a broad scientific program over the energy range from thermal to about seven hundred MeV. Largely because of the increased intensity over such an unprecedented energy range, use of these two facilities for nuclear science research has grown from 36 experimenters in 1987 to 118 in 1990. This paper focuses on research underway or recently completed at the high-energy neutron source of the WNR facility.

1. INTRODUCTION

The WNR facility at Los Alamos National Laboratory consists of three flight paths at target-1 of the Los Alamos Neutron Scattering Center (LANSCE); target-2, a low-current target-area with an external proton beam capability, and target-4, a high-energy white neutron source. All of these areas are driven by 800 MeV proton beam from the Clinton P. Anderson Los Alamos Meson Physics Facility (LAMPF) which can be multiplexed to both target-1 and target-2 or target-4 allowing simultaneous operation [1]. Because the target-1 source is designed for experiments using low-energy neutron production, this paper will only address the features and recent research at target-4.

The target-4 facility provides neutrons over the energy range from approximately 100 keV to above 750 MeV. This is done by bombarding a heavy-metal target with pulsed 800 MeV proton beam from LAMPF to produce spallation neutrons. The production target is a 3-cm diam by 7.5-cm long water-cooled cylinder of tungsten located in a 1.8-m diameter x 1.2-m high vacuum chamber which is contained in a massive shield of iron and concrete with penetrations for seven neutron beamlines. Each penetration has a remotely controlled, removable mechanical shutter mechanism to turn off the neutron beam to its flight path and to provide some initial neutron collimation. Downstream of the shutter there is additional collimation and permanent magnets to deflect contaminant charged particles. All flight paths have one or more detector stations allowing six experiments to operate simultaneously. Data is acquired with CAMAC-based MicroVax data acquisition systems. A plan view of the WNR Facility, highlighting features of the target-4 spallation source is shown in Fig. 1.

2. PROTON BEAM

Beam for WNR is chopped at the LAMPF injector into a pulse approximately 20-ns long containing 3×10^8 protons and bunched into the phase acceptance of the accelerator. Proton pulse separations can be adjusted in 360 ns increments but typically are set between 1 and 4 microseconds depending on the frame-overlap requirements of WNR experiments. After acceleration the beam consists of a train of micropulses approximately 60 ps wide contained in a macropulse envelope extending for ~ 800 microseconds. As many as 70 macropulses/s are available from LAMPF (at a spacing of 1 μs this would give 56,000 micropulses/s and 2.7 μa beam on target). At the present time pulsed magnet limitations in the LAMPF beam transport system restrict the WNR to a maximum of 60 macropulses/s. The proton pulse disperses after acceleration to a time width of approximately 150 ps at the WNR target. There are two non-intercepting wall-gap beam-pulse monitors [2] located along the proton beam line and separated by about 300 meters. These are available to measure the proton beam energy and charge, measure the pulse-to-pulse amplitude variation of the beam which is needed to properly perform a deadtime correction in high rate experiments, and as pulsed beam diagnostics. The principal one used by experimenters is mounted about 23-m upstream of the center of target-4 and is used to provide a precise timing fiducial. The beam current is measured with a high-sensitivity toroid located near center of target-2 (see Fig. 1). A monitor detector at a flight path of 7 meters at an angle of 90° to the neutron production target is used by linac operators to adjust the beam position and size for optimum neutron output and by experimenters as a relative neutron flux monitor.

3. EXPERIMENTAL FACILITIES

In addition to the monitor flight path, there are six neutron beam lines with lengths between 8 and 90 meters. The beamlines are arranged at angles realtive to the proton beam between 15° and 90° and provide some tailoring of the neutron spectrum for different experiments . The 90 deg., flight paths are more suited to low-energy experiments because the neutron flux drops rapidly above about 100 MeV, lower energy neutrons are attenuated less by the target, and the flight path uncertainty is smallest. At 15 deg. the neutron spectrum extends to nearly 750 MeV and lower energy neutrons are more strongly absorbed by the target, resulting in a 'harder' spectrum. Flight path lengths, experiment station locations, and some examples of recent experiments are given in Table 1. The maximum possible length of each flight path is shown in curly brackets and information about facilities under construction is in square brackets.

Table I. WNR Target-4 Flight Paths

Angle	Station Distance (m)	Recent Experiments
90L	8	0 to 30 MeV (n,p), (n,d), etc.
30L	[20] 40 {250}	3 to 750 MeV σ_t; (n,xγ); (n,p)
15L	90 {250}	30 to 350 (n,p), (n,d)
15R	11	(n,g); (n,xγ); n-p Bremsstrahlung
30R	[20] {40}	Defense program detector calibration
60R	20 {40}	$\sigma_f(E_n,\theta_f,m_f)$, 0.5 - 400 MeV(n,f)
90R	7 {20}	Facility neutron monitor
0	40 250	800 MeV (n,f), (p,n),

Several experiments have recently been performed on each flight path to determine the outgoing neutron spectrum. Measurements on 60R [3] and 15L [4] have used neutron scattering from hydrogen as a standard, whereas all of the others (15L, 30L, and 90L) have used new fission cross section data [3] from WNR for either ^{238}U(n,f) or ^{235}U(n,f) to determine the neutron flux over the range from 3 - 250 MeV. Above 250 MeV the measurements assume that the fission cross section is roughly independent of energy and has about the same value as at 250 MeV. This assumption is based on the shape of high-energy neutron and proton-induced fission data supplemented by a measurement of the high-energy fission cross section using a plastic scintillator and a calculated efficiency [3]. A comparison of measured and calculated [5] neutron spectra is shown in Fig. 2. Because of the difficulty in determining proton beam current, the spectra were normalized to the intra-nuclear cascade (INC) model predictions over the region near 10 MeV where previous measurements and calculations have shown good agreement. The calculations are for the WNR as-built tungsten target, including the stainless steel cladding and water jacket. Two independent measurements performed on the 15L and 15R flight paths are shown in Fig. 2, have the same relative normalization and are in excellent agreement with each other.

In addition to the target-4 'white' source, a nearly monoenergetic neutron beam is also available [6]. Neutrons are produced with an energy spread of about 1 MeV at a reaction angle of 0^{o} via the $^{7}Li(p,n)$ reaction. This source can be used simultaneously during target-4 operation with a loss of intensity at target-4 of less than 10%. In some cases, WNR can operate at energies as low as 256 MeV, producing lower energy monoenergetic beams. There is a detector station at a flight path of 250 m for these experiments (see Fig. 1).

4. RESEARCH PROGRAM

The advent of the target-4 source at WNR has made it possible to perform exclusive experiments with neutrons at energies higher than has been previously possible. Those studies are enhancing our knowlege of such neutron-induced phenomena as fission, photon and charged-particle production, and scattering. The organization of this section will be to provide a brief description of the experimental program underway on each of the flight paths either during the previous operating period or planned for 1991.

4.1 90L Flight Path

This flight path and the corresponding one at 90R have the most advantageous spectra for experiments at low energy (< 50 MeV). Here experimenters [7] have developed a system for measuring (n,p) and (n,a) reaction cross sections, angular distributions, and charged-particle spectra from threshold to about 30 MeV in order to infer nuclear level density information about both residual nuclei and the target nucleus.

By measuring charged-particle emission spectra and comparing the shape of the spectra for a given neutron energy with Hauser-Feshbach calculations, level densities of the residual nucleus can be inferred. Such calculations take level densities of the residual nucleus as input and vary the level density until a good representation of the data is obtained. Once those data are obtained as a function of energy, the analysis can address questions such as: is the level density is a function of incident neutron energy; can spin-cut off parameters be derived from such data at different incident energies; and where is the onset of precompound processes. The second technique involves measuring the excitation function for the high-energy end of the charged-particle spectrum. Since the optical model transmissions change slowly, the decay width of the compound nucleus through these channels changes slowly (and can be calculated). The denominator in the Hauser-Feshbach formula changes much more rapidly because in many cases it is dominated by neutron decay channels. At an excitation energy 1 to 2 MeV below the ground state, that width is dominated by the level density in the target nucleus and can therefore be obtained by measuring the magnitude of the charged-particle emission cross section. At present the experiment is analyzing results for $^{27}Al(n,\alpha)$, for $^{28}Si(n,\alpha)$ and (n,p) to resolved final states, and Fe(n,α). Additional reaction cross section data with a wide range of applications ranging from neutron thetapy to neutron heating of fusion materials has been taken for $^{10}B(n,\alpha)$ and C(n,α) . In a complementary measurement, this group also measured the total cross section of ^{28}Si with high-energy resolution at the 90-meter station of the 15L flight path in order to derive level densities in the compound nucleus, ^{29}Si.

4.2 30L Flight Path

At the 40-m station of this flight path, there were two experimental programs which shared beam time during the past operating period. One was a series of high-resolution measurements [8] of individual lines from (n,xγ) reactions for neutron energies extending to energies of about 100 MeV for a wide variety of targets ranging from ^{56}Fe to ^{207}Pb. Those studies utilized a germanium detector and converted the gamma-ray yield information to cross sections using measured and calculated efficiencies and the neutron flux obtained using a ^{238}U fission chamber. The final data contained a vast amount of information about complex reaction processes, including signatures of (n,xn) reactions. The latter results are particularly useful for applications such as accelerator shielding and are needed to build up a data base that will permit detailed testing and therefore improvement of the nuclear models presently used in this energy range.

The second experiment on this flight path involved a measurement of the neutron total cross section for energies from 4.5 to about 600 MeV [9]. In this experiment, a highly collimated 2.54-cm diam neutron beam was used to measure neutron transmission as a function of energy for samples located in a computer-driven changer positioned at a distance of about 12 m from the neutron source. About twenty nuclei ranging in A from Be to Bi were used. At the 40-m station, neutrons were detected by a small fast-plastic scintillation counter preceeded by a veto detector. Systematic errors were minimized using a rapid sample-changing technique and highly precise (1% statistical uncertainty in 1% energy bins or better) data were obtained. Particular emphasis was given to isotopically separated samples of closed-shell nuclei such as ^{40}Ca, ^{90}Zr, and ^{208}Pb for which a substantial body of intermediate-energy proton scattering data already exists. The results are being analyzed to investigate energy-dependent isovector effects in in terms of Schroedinger and Dirac optical potentials.

Using the same flight path during the previous two years, a collaboration from Los Alamos, the University of New Mexico, and the University of Colorado was involved in measurements of neutron-induced pion production on samples of

C, Al, Cu, and W from 200 to 600 MeV [10]. Those data are among the first results to separate π^+ and π^- production cross sections and they provide valuable information needed to test intra-nuclear cascade predictions. The experimental set-up for those measurements used a magnetic spectrometer which covered the neutron energy range from 200 to 600 MeV and detected pions at angles ranging from 25° to 125°. Production cross sections for π^+ and π^- were obtained by reversing the polarity of the spectrometer magnet. Some of the results for C(n,π^-) are shown in Fig. 3 over ther range from 212 to 562 MeV and an angle of 25°.

4.3 15L Flight Path

Except at few discrete energies, studies of (n,p) charge-exchange processes have been relatively slow to develop compared to those of (p,n) because of the lack of suitable neutron sources and detector systems. The physics involved is highly complementary to that in (p,n) studies, and in some cases is simpler to interpret because isovector (n,p) To +1 excitations occur at lower energies than in (p,n) reactions and have a larger coupling coefficient.

Over the past four years the 15L flight path has been developed [4] for studies of medium-energy (n,p) charge-exchange reactions with the general goals of calibrating the $T^>$ Gamow-Teller strength with respect to measured β^- decay in several p-shell nuclei, and in the only fp shell nucleus where this is possible, ^{64}Ni; and to study the energy dependence of the Gamow-Teller cross sections in several nuclei in order to compare those cross sections to calculations based on effective nucleon-nucleus interactions and nuclear structure.

A schematic drawing of the detection apparatus is shown in Fig. 4. The neutron beam enters from the left and froward-angle (n,p) cross sections are measured by bending the protons out of the neutron beam with a dipole magnet into a CsI(Tl) array. A multiple target array was used to increase the data rate. Four targets, separated by multi-wire proportional counters were used with two redundant charged-particle veto counters ahead of the first target. The scattering angle was measured by two (x,y) drift chambers located downstream of the target array. The CsI array consisted of fifteen 7.62 x 7.62 x 15.24 cm^3 crystals stacked in an array five wide and three high and capable of stopping up to 250 MeV protons. The scattering angle was measured using two large drift chambers immediately in front of the CSI array.

Some results from this program have been recently submitted for publication [11,12]. Fig. 5 shows typical double-differential cross section data obtained for ^{6}Li(n,p), ^{12}C(n,p), and ^{13}C(n,p). The data for Fig. 6 was taken from an experiment [13] on ^{32}S(n,p) and is an excellent example of the power of a white source for this type of experiment. There the cross section is plotted as a function of the incident neutron energy and excitation energy of the residual nucleus. The white source allows examination of the details of the reaction mechanism such as the evolution of giant resonances with energy in exquisite detail.

4.4 15R Flight Path

During the past year this flight path was used in an experiment to measure three-point angular distributions from $^{40}Ca(n,\gamma)$ in a search for additional evidence for the existence of the isovector giant quadrupole resonance in ^{41}Ca. This experiment used a 10-cm diam by 15-cm long BGO crystal inside an active plastic scintillator used to veto cosmic ray and escape events. Preliminary results of this work were presented at the Fourth International Workshop on Radiative Capture [14].

A major new physics initiative at the WNR is a program to study the gamma emission following neutron-proton scattering (neutron-proton bremsstrahlung or NPB) [15]. The goal of this experiment is to study the effects of meson-exchange currents in the nucleon-nucleon interaction over a wide range of inelasticities. Such effects are expected from theory to be large but have not yet been measured in detail. Of additional interest in this experiment is the expectation that the results will contribute to the understanding of the source of high-energy gamma rays observed in heavy-ion reactions. The experiment will have three phases. First, the inclusive gamma-production cross section will be measured for incident neutron energies between 50 and 400 MeV using a liquid hydrogen target. A gamma-ray telescope with an active converter, two delta-E detectors and a large volume calorimeter will be used. The second phase will add a segmented array of proton detectors in order to measure proton-gamma coincidences and define NPB events. Finally, in the third phase an array of neutron detectors will be added to measure the full neuron-proton-gamma coincidence.

4.5 60R Flight Path

From 1987 to 1989 this flight path was used in the program of intermediate-energy fission cross section measurements discussed in detail in another contribution to this conference [16]. Starting in 1990, a new set of measurements [17] was begun to determine temperature dependent effects in neutron-induced fission. In the first segment of this experiment, a low-mass chamber containing two 19-element 3 x 3 cm^2 PIN diode arrays was used to detect fission fragments from 2 to 200 MeV neutron-induced fission of ^{238}U. The fragment energy was determined by comparison with measurements of fragments from spontaneous fission of ^{252}Cf. Using momentum conservation and correcting for neutron emission and energy loss in the foil, the experiment was able to get the $^{238}U(n,f)$ fragment energies and mass distribution.

Starting in the summer of 1991 the chamber will be surrounded by an array of seven liquid scintillators. By detecting neutrons in coincidence with fission fragments, the experiment will obtain multiplicities of neutrons evaporated prior to fission and multiplicities of neutrons emitted from the fragments. These data will be used to provide insight into the effects of shells and nuclear dissipation on the probability of fission.

5. CONCLUSIONS

The program discussed in this paper touches only on the highlights of measurements at the WNR target-4. Roughly equivalent amounts of work have been done at target-1 and target-2 with low-energy neutrons and incident proton beams respectively. For 1991, the number of proposals for research have expanded over those for 1990 and include proposed work to investigate cross sections for energetic neutrons incident on biological materials and on shielding materials of interest to the United States Space Exploration Initiative, measurements associated with the Los Alamos transmutation of radioactive waste program [18], H(n,p) elastic scattering cross section measurements up to 50 MeV, and nineeteen other experiments. The WNR target-4 facility together with targets-1 and -2 are proving to be valuable and versatile tools which to some extent have revived interest in neutron-based nuclear science research in the United States.

1. P. W. Lisowski, C.D. Bowman, and S. A. Wender: "The Los Alamos National Laboratory Spallation Neutron Sources", Nucl. Sci and Eng., **106**, 208 (1990).
2. D. A. Lind: "Charge-Exchange Studies at the Los Alamos Meson Physics Facility - Weapons Neutron Research Facility", Can. J. Phys., **65**, 637 (1987).
3. P. W. Lisowski *et al.*: "Fission Cross Sections in the Intermediate Energy Range", These proceedings.
4. D. S. Sorenson: "The Energy Dependence of the T> Gamow-Teller Strength in p-shell Nuclei Observed in the (n,p) Reaction", Ph.D. Thesis, University of California at Davis, (1990).
5. R. E. Prael and Henry Lichtenstein: "User Guide to LSC: The LAHET Code System", LA-UR-89-3014, Los Alamos National Laboratory, (1989).
6. R. G. Jeppeson: "Observation of the Gamow-Teller and Fermi Strength in Light Nuclei Using the 800 MeV (p,n) Reaction", Ph.D. Thesis, University of Colorado, Boulder, CO. (1987).
7. R. C. Haight: "Nuclear Level Densities Through (n,p) and (n,alpha) Reactions", FIN-91-ER, Los Alamos National Laboratory, p 343, (1991).
8. D. C. Larson *et al.*: "White Source Gamma-Ray Production Spectral Measurement Facilities in the US", Proc. International Conference on Nuclear Data for Science and Technology, Julich, Germany, To be published (1991).
9. R. Finlay *et al.*: "Neutron Total Cross Sections at Intermediate Energies", Proc. International Conference on Nuclear Data for Science and Technology, Julich, Germany, To be published (1991)
10. M. Brooks *et al.*, "Measurements of Pion-Production Cross Sections on C, Al, Cu, and W by 200 - 600 Neutrons", BAPS Vol. 36, No 4, 1299, (1991).
11. A. Ling *et al.*: "Ground State Gamow-Teller Strength in ^{64}Ni(n,p)^{64}Co Cross Sections at 90-240 MeV, Submitted to Phys. Rev., (1991).
12. D. S. Sorenson *et al.*: "The Energy Dependence of the Gamow-Teller Strength in p-shell Nuclei Observed in the (n,p) Reaction", submitted to Phys. Rev. Lett., (1991)

13. B. K. Park: "Spin and Non-spin Resonances from the (n,p) Reaction on ^{40}Ca and ^{32}S for Incident Energies of 50-250 MeV, Ph.D. Thesis, Ohio University, Athens, Ohio, (1991)
14. C. A. Laymon et al.: "Giant Resonance Studies Through Neutron Capture", LA-UR-91-1086, Los Alamos National Laboratory Report to the Department of Energy, Summaries for 1990, (compiled by P. W. Lisowski), (1991).
15. Lectures from the Workshop on Nucleon-Nucleon Bremsstrahlung, (Compiled by B. F. Gibson, M. E. Schillaci, and S. A. Wender), LA-11877-C, Los Alamos National Laboratory, (1990).
16. P.W. Lisowski *et al.* "Fission Cross Sections in the Intermediate Energy Range", These proceedings.
17. A. Gavron *et al.*: "Properties of Neutron Induced Fission on ^{238}U", LA-UR-91-1086, Los Alamos National Laboratory Report to the Department of Energy, Summaries for 1990, (compiled by P. W. Lisowski), (1991).
18. P. W. Lisowski, C. D. Bowman, E. D. Arthur, and P. G. Young, "Nuclear Physics Information Needed for Accelerator Driven Transmutation of Nuclear Waste", Proc. International Conference on Nuclear Data for Science and Technology, Julich, Germany, To be published (1991).

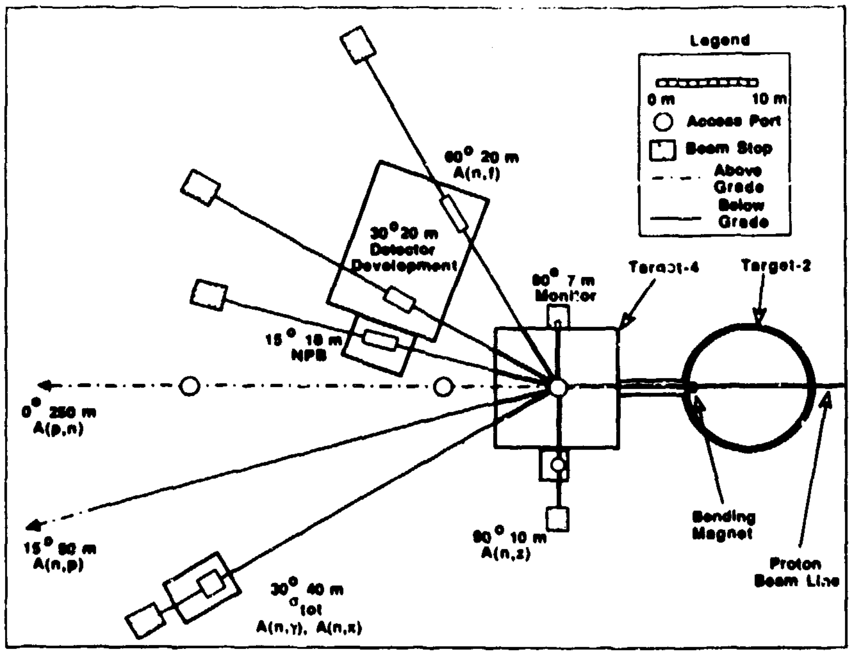

Fig. 1 Layout of the WNR target-4 facility. The proton beam enters from the right. Flight paths and detector stations associated with other facilities at WNR were omitted from this drawing for clarity.

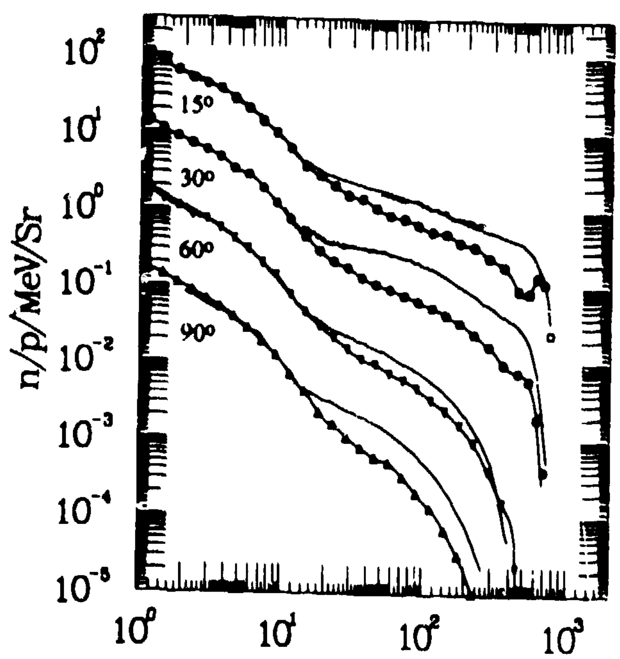

Fig. 2 Calculated and measured spectra for the WNR tungsten target. The curves with symbols show the results of INC calculations. The other lines are drawn through the measurements. To offset the curves, the 15° results have been multiplied by 1000, the 30° results by 100, and the 60° results by 10.

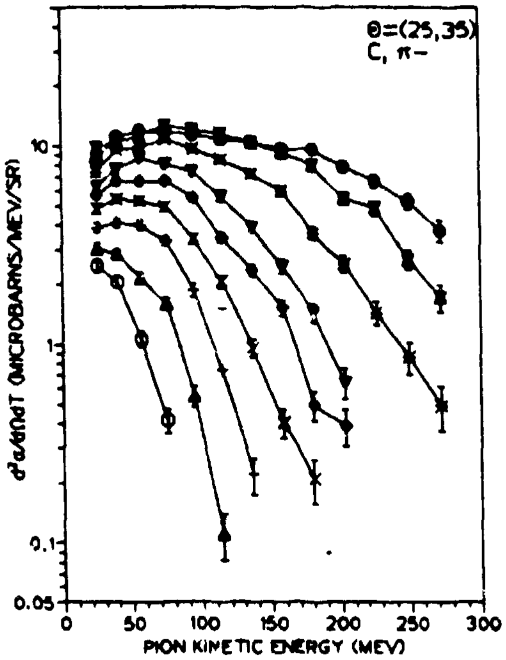

Fig. 3 Measured π^- production cross sections at an angle of 25° for incident neutrons from .:00 to 600 MeV.

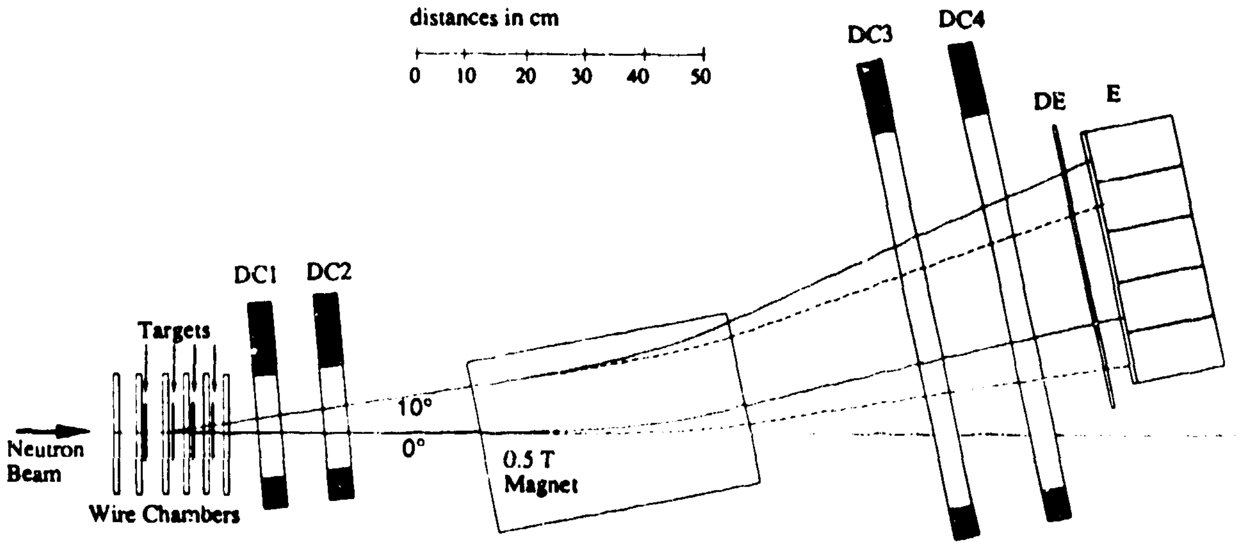

Fig. 4 Detection system for the (n,p) measurements on the 15L 90-m flight path at WNR. The proton beam enters from the left producing reactions in targets T1 - T4. Charged particles are swept out of the beam by the magnet.

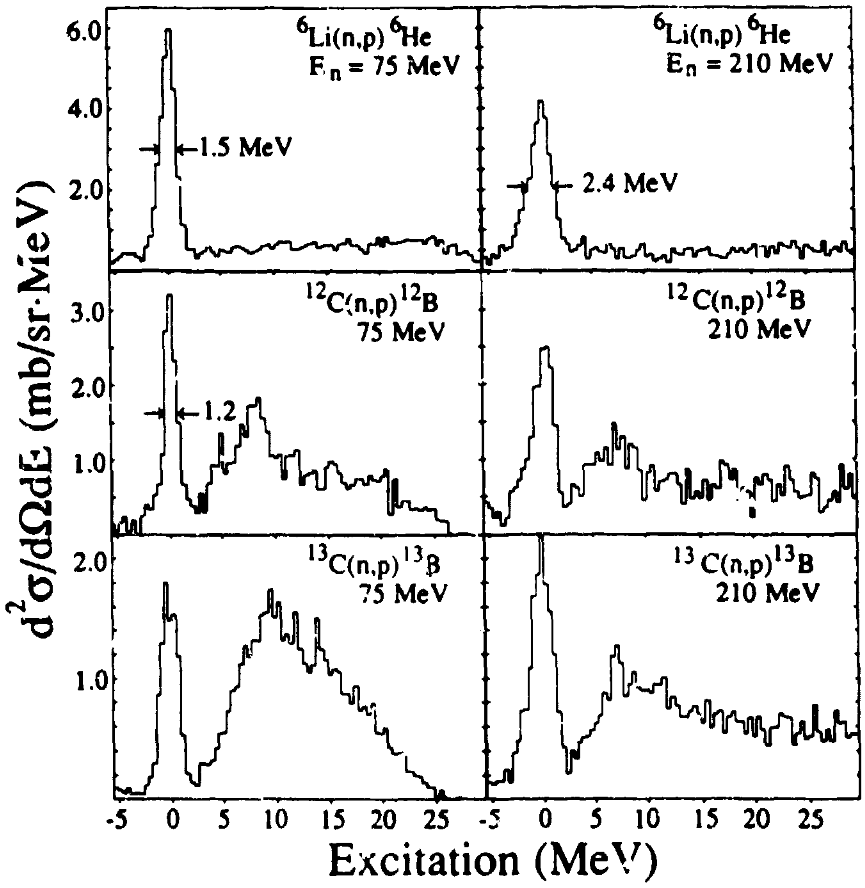

Fig. 5 Double-differential cross section results obtained with the (n,p) detection system at WNR for ^{6}Li(n,p), ^{12}C(n,p), and ^{13}C(n,p).

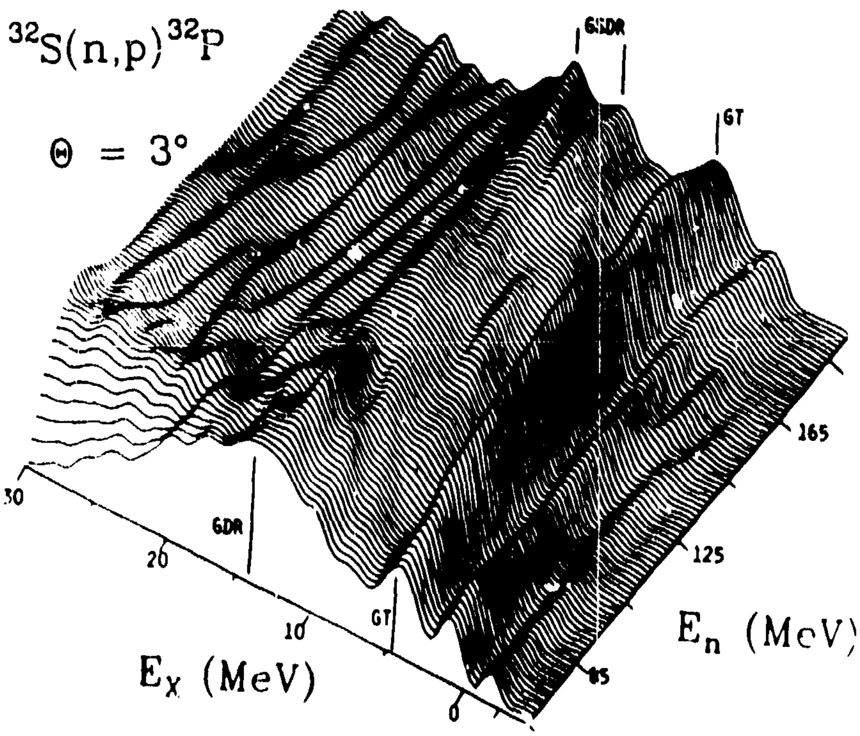

Fig. 6 Excitation energy versus incident neutron energy for the ^{32}S(n,p) reaction. The curves represent a small part of the data obtained in a single measurement at the WNR. These results illustrate the capability of the white source to show the energy evolution of the cross section over the entire energy range of the measurement. The markers indicate the locations of the Gamow-Teller, Dipole and Spin Dipole resonances.